Published in final edited form as:

Toxicol Appl Pharmacol. 2015 June 1; 285(2): 136–148. doi:10.1016/j.taap.2015.03.029.

Glutathione *S*-transferase P protects against cyclophosphamide-induced cardiotoxicity in mice

Daniel J. Conklin[1,2], **Petra Haberzettl**[1,2], **Ganapathy Jagatheesan**[1,2], **Shahid Baba**[1,2], **Michael L. Merchant**[1,3], **Russell A. Prough**[1,4], **Jessica D. Williams**[5], **Sumanth D. Prabhu**[6], and **Aruni Bhatnagar**[1,2,4]

[1]Diabetes and Obesity Center, University of Louisville, Louisville, KY 40292

[2]Institute of Molecular Cardiology, University of Louisville, Louisville, KY 40292

[3]Division of Nephrology, Department of Medicine, University of Louisville, Louisville, KY 40292

[4]Department of Biochemistry and Molecular Biology, University of Louisville, Louisville, KY 40292

[5]University of Cincinnati College of Medicine -- Internal Medicine Cincinnati, OH 45267

[6]Division of Cardiovascular Disease University of Alabama-Birmingham, Birmingham, AL 35294

Abstract

High-dose chemotherapy regimens using cyclophosphamide (CY) are frequently associated with cardiotoxicity that could lead to myocyte damage and congestive heart failure. However, the mechanisms regulating the cardiotoxic effects of CY remain unclear. Because CY is converted to an unsaturated aldehyde acrolein, a toxic, reactive CY metabolite that induces extensive protein modification and myocardial injury, we examined the role of glutathione *S*-transferase P (GSTP), an acrolein-metabolizing enzyme, in CY cardiotoxicity in wild-type (WT) and GSTP-null mice. Treatment with CY (100-300 mg/kg) increased plasma levels of creatine kinase-MB isoform (CK·MB) and heart-to-body weight ratio to a significantly greater extent in GSTP-null than WT mice. In addition to modest yet significant echocardiographic changes following acute CY-treatment, GSTP insufficiency was associated with greater phosphorylation of c-Jun and p38 as well as greater accumulation of albumin and protein-acrolein adducts in the heart. Mass spectrometric analysis revealed likely prominent modification of albumin, kallikrein-1-related peptidase, myoglobin and transgelin-2 by acrolein in the hearts of CY-treated mice. Treatment with acrolein (low dose, 1-5 mg/kg) also led to increased heart-to-body weight ratio and myocardial contractility changes. Acrolein induced similar hypotension in GSTP-null and WT mice. GSTP-null mice also were more susceptible than WT mice to mortality associated with high-dose acrolein (10-20 mg/kg). Collectively, these results suggest that CY cardiotoxicity is

Address Correspondence to: Daniel J. Conklin, Ph.D. Diabetes and Obesity Center University of Louisville 580 S. Preston Street Delia Baxter Building, Rm. 404E Louisville, KY 40292 FAX: (502) 852-3663 Ph: (502) 852-5836 dj.conklin@louisville.edu.

5. No disclosures.

regulated, in part, by GSTP, which prevents CY toxicity by detoxifying acrolein. Thus, humans with low cardiac GSTP levels or polymorphic forms of GSTP with low acrolein-metabolizing capacity may be more sensitive to CY toxicity.

Graphical Abstract

Cyclophosphamide (CY) treatment results in P450-mediated metabolic formation of phosphoramide mustard and acrolein (3-propenal). Acrolein is either metabolized and detoxified by glutathione S-transferase P- (GSTP) via conjugation with GSH or acrolein can react with circulating and cardiac proteins to form protein-acrolein adducts that may contribute to cardiac injury, increased vascular permeability and edema and acute cardiotoxicity. Under low dose exposure, this event is reversible but at high levels of CY treatment and/or in susceptible individuals (e.g., *hGSTP1* polymorphism), CY-induced cardiotoxicity is augmented and sudden death may occur.

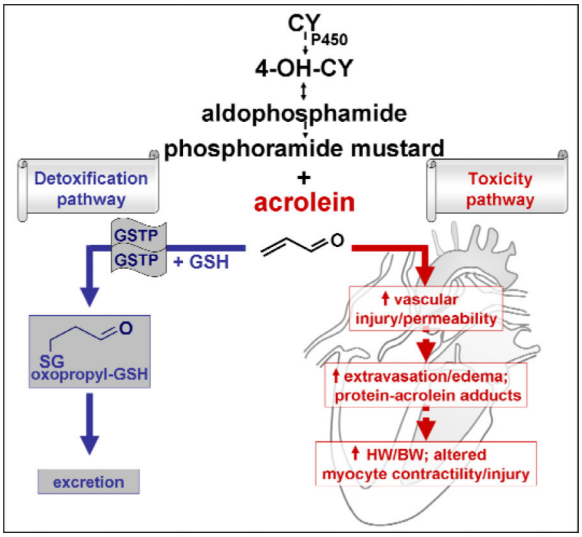

Keywords

acrolein; apoptosis; cardiotoxicity; Cytoxan; GSTP1; JNK/c-Jun

1. Introduction

Cyclophosphamide (CY; Cytoxan®) is a widely used anti-neoplastic drug for the treatment of lymphomas, brain cancer and leukemia, and as a preparatory treatment for bone marrow transplant (Worth *et al.*, 1999; Kuittinen *et al.*, 2005; Morandi *et al.*, 2005). Because of its immunosuppressive activity, it is also frequently used for the treating autoimmune diseases, amyloidosis, idiopathic nephritis, severe rheumatoid arthritis and multiple sclerosis (Perini *et al.*, 2007; Sharda *et al.*, 2008). Several of these treatment regimens require high doses of CY that are associated with significant side effects such as bone marrow suppression, and hemorrhagic cystitis that vary in incidence, manifestation and severity (Shepherd *et al.*, 1991). However, some of the most serious side effects of high dose CY-containing regimens are associated with the acute cardiotoxic effects of the drug that usually manifest as

endothelial damage followed by extravasation of toxic metabolites, and myocyte damage leading to diastolic contractile dysfunction (Drimal *et al.*, 2006; Zver *et al.*, 2008; Senkus and Jassem, 2011). Frequent occurrences of acute fulminant congestive heart failure, hemorrhagic myopericarditis and sudden death have also been reported (Morandi *et al.*, 2005; Senkus and Jassem, 2011). Even though cardiac complications of CY therapy have declined due to recent adoption of multifractionated schedule of administration, the incidence of the cardiotoxic effects of CY treatment remains high. High dose CY infusion induces reversible stage 3 heart failure in 10% of metastatic breast cancer patients with a median decline in ejection fraction of 31% (Gil-Ortega and Carlos Kaski, 2006); and nearly 40% of patients undergoing pediatric allogenic hematopoietic stem cell transplantation treated with high dose CY experience cardiac complications (Motoki *et al.*, 2010). In adult populations treated with CY, mortality rates up to 20% (breast cancer trial) have been reported (Morandi *et al.*, 2005). Nevertheless, the mechanism of CY cardiotoxicity remains unclear, and there is an urgent need to better understand the acute cardiac effects of CY in order to treat or minimize cardiotoxicity of high dose CY chemotherapy.

CY is a pro-drug that is metabolically converted by cytochrome P450 into highly reactive metabolites - phosphoramide mustard, which forms DNA crosslinks and induces cell death in proliferating cells. Metabolism of CY also generates acrolein (Ludeman, 1999), and acrolein is implicated in the urotoxic, nephrotoxic and neurotoxic effects of CY (Cox, 1979; Low *et al.*, 1982; Levine and Richie, 1989; Giraud *et al.*, 2010). Urinary acrolein concentrations are increased in CY-treated patients (Al-Rawithi *et al.*, 1998; Takamoto *et al.*, 2004) and treatment with thiol containing compounds such as amifostine and MESNA protects against CY-induced bladder toxicity (Bryant *et al.*, 1980; Roberts *et al.*, 1994; Batista *et al.*, 2007), suggesting that acrolein may be a significant mediator of CY toxicity.

Acrolein is an unsaturated aldehyde that readily reacts with cellular nucleophiles such as glutathione and cysteine and histidine side chains of proteins. As a reactive electrophile, acrolein is highly toxic when administered to perfused rat hearts, isolated coronary blood vessels, or incubated with cardiac myocytes and isolated cardiac mitochondria (Toraason *et al.*, 1989; Biagini *et al.*, 1990; Sklar *et al.*, 1991; Conklin *et al.*, 2001). Acrolein toxicity could be attributed to the high reactivity of the α,β–unsaturated structure of the aldehyde, because addition of nucleophiles such as glutathione to the site of unsaturation attenuates acrolein reactivity and toxicity. Although acrolein reacts spontaneously with glutathione, this reaction is catalyzed by glutathione *S*-transferase P (GSTP) increasing the rate (600-fold) of conjugation of acrolein with GSH (Berhane *et al.*, 1994). Thus, enzymatic conjugation by GSTP facilitates and enhances the detoxification and removal of acrolein and other related aldehydes (Berhane *et al.*, 1994). Our previous studies have shown that GSTP protects against endothelial dysfunction induced by inhaled acrolein or tobacco smoke, which contains high levels of acrolein, and against CY-induced urotoxicity (Conklin *et al.*, 2009a; Conklin *et al.*, 2009b) -- both conditions reflecting the high sensitivity of endothelium to acrolein. Nevertheless, it is unclear whether CY-induced cardiotoxicity is affected by GSTP-mediated acrolein metabolism. Therefore, we designed the current study to examine the role of GSTP in regulating acute cardiac effects of high-dose CY, because clinical studies show that high-dose CY toxicity occurs during or soon after CY

administration (Morandi *et al.*, 2005). We observed greater cardiac permeability and toxicity of CY in GSTP-null than in WT mice, indicating that GSTP activity in coronary endothelium and myocytes is likely an important determinant of CY cardiotoxicity. Because polymorphic forms of human *GSTP1* differ in their ability to metabolize acrolein (Pal *et al.*, 2000), these findings have important implications in individualizing high dose CY treatment and developing safer and more effective strategies for preventing the cardiotoxic effects of high-dose CY therapy.

2. Methods

2.1. Animal Studies

Glutathione *S*-transferase-P1/P2 null mice were generated on a 129xMF1 background using homologous recombination (Henderson *et al.*, 1998) and were bred onto a B/6 background. Littermates of $GSTP^{(-/-)}$ (GSTP-null) and $GSTP^{(+/+)}$ (GSTP wild-type, WT) obtained from Drs. C. Henderson and R. Wolf (Univ. Dundee) were maintained as independent lines. Both WT and GSTP-null mice (male, 10-16 weeks old) were treated in accordance with the Declaration of Helsinki and the Guide for the Care and Use of Laboratory Animals as adopted and promulgated by the U.S. National Institutes of Health and approved by the University of Louisville IACUC. To examine CY cardiotoxicity, WT and GSTP-null mice were treated with saline (control; 0.1 ml, ip) or 100, 200 and 300 mg/kg CY (Sigma-Aldrich, USA), which is within the dose range of high dose CY therapy in humans (4-7 g/m^2) as adjusted for mice, i.e., 25 mg/kg human = 300 mg/kg mice (Freireich, 1997; Morandi *et al.*, 2001; Zver *et al.*, 2007). To examine direct effects of acrolein, a dose range of 1-5 mg/kg acrolein (ip; po) was used in initial studies because there was neither mortality nor weight loss in either WT or GSTP-null mice in this dose range. In lethality studies, mice were treated with water or acrolein (Sigma-Aldrich; 0.1 ml; po; 5, 10 or 20 mg/kg) in water or injected (0.1 ml, ip) with saline or acrolein (1, 3, 10 or 20 mg/kg in saline). In all studies, each mouse received only a single dose of either CY or acrolein.

2.2 Cardiovascular toxicology

2.2.1 Blood pressure—Cardiovascular effects (i.e., heart rate, systolic, mean, and diastolic blood pressure) of acrolein or CY treatment were measured by non-invasive pressure-volume tail cuff methodology (CODA6; Kent Scientific, Torrington, CT, USA) at 1, 4 or 24h after dosing. For blood pressure measurements, mice were acclimated for 5 or more days to gentle heating and brief confinement (<30 min) in hooded, plexiglass tubes.

2.2.2 Echocardiography—Echocardiography in 2-dimensional M-mode was performed in anesthetized male mice (12-16 weeks old) at baseline (i.e., saline control and up to 1 week before treatment) and post-treatment (1h or 4h) using either a Philips Sonos 5500 Ultrasound System (Avertin, 0.25 g/kg bwt; acrolein treatment) or a VisualSonics Vevo 770 (2 % isoflurane; CY treatment). The echocardiograms (e.g., short and long axis, M-mode, Doppler: aorta and mitral valve) were analyzed using Philips software or VisualSonics Cardiac Measurement Package (Ver. 17), respectively. Representative echocardiograms (speed: 1/5, length: 4 loops) pre- (BSL) and 1h post-acrolein are provided in a supplemental online video.

2.3. Biochemical analyses

Following indicated treatments, mice were euthanized (sodium pentobarbital, 40 mg/kg bwt) and blood was collected in Na_4·EDTA (0.2 M; 16 μl/ml blood) *via* cardiac puncture. Plasma was separated (2,000×*g*, 20 min, RT) and used to measure albumin (bromocresol green; Wako, Richmond, VA, USA), CK and CK·MB (ThermoElectron, Fremont, CA, USA) using a Cobas-Mira Plus Clinical Analyzer (Roche). Cardiac wet weight (nearest mg) was measured, a mid-LV cross-section was formalin-fixed (10% neutral buffered formalin, NBF) and the rest of heart was snap-frozen (stored at −80 °C).

Tissue levels of glutathione (reduced GSH) and thiobarbituric acid (TBARS) were measured in heart, stomach, kidney and liver according to previously published methods (Srivastava *et al.*, 2002). Cardiac expression of GST A (α), M (μ), and P (π) were analyzed by Western blot using commercially available antibodies (Pope *et al.*, 2008). Total GST conjugating activity toward substrates, 1-chloro-2,4-dinitrobenzene (CDNB; 1 mM) and ethacrynic acid (EA; 200 μM), was measured in cardiac homogenates (Habig *et al.*, 1974). Cardiac albumin, CY-induced phosphorylation of JNK, c-Jun, p38, p44/42, Casp3 activation and cardiac abundance of protein-acrolein adducts were measured by Western blotting as previously described (Conklin *et al.*, 2009a). Briefly, cardiac proteins were separated by SDS-PAGE and transferred to PVDF membranes (Bio-Rad, Hercules, CA, USA). Membranes probed with antibodies against albumin (1:1000, Bethyl, Montgomery, TX, USA), Casp3, GAPDH or phosphorylated and total SAPK/JNK, c-Jun, p42/44 (ERK1/2), p38 (1:1000, Cell Signaling Technology, Danvers, MA, USA) or with IgG-purified rabbit polyclonal antibody against KLH-acrolein (Keyhole Limpet Hemocyanin, raised in house) were developed using ECL® plus reagent (Amersham Biosciences, Piscataway, NJ, USA). Band intensities were detected with a Typhoon 9400 variable mode imager (Amersham Biosciences) and quantified using Image Quant TL software (Amersham Biosciences). Total protein, GAPDH detection or amido black stains were used as loading controls.

2.3.1 Protein Modification and Identification—Whole cardiac lysate (600-700 μg) was immunoprecipitated using IgG-purified protein-acrolein antibody (3-5 μg) and Sepharose A. Protein in RIPA buffer was loaded on a 2.5% polyacrylamide gel and run for 5 min to dilute buffer. Protein was stained with Coomassie blue, and approximately 0.5 mL portions of the Coomassie-blue stained agarose gel band were excised and de-stained using sequential washes of 0.1M triethylammonium bicarbonate, pH 8.5 (TEA-BC) and 100% methanol. The gel bands were digested with 1 μg Arg-C protease (Sigma, St. Louis, MO) without reduction and alkylation overnight at 37 °C. The supernatant was used for LC-MS analysis. The gel plug was then reduced and alkylated using a modification of Jensen's method (Jensen*et al.*, 1997) and as previously described (Vladykovskaya *et al.*, 2012), and digested overnight at 37 °C using 2 μg mass spectrometry grade trypsin (Promega, Madison, WI). The digest supernatants were trap-cleaned (Michrom C18 Peptide MacroTrap, Michrom Bioresources Inc, Auburn, CA), then fractionated by strong cation exchange (SCX MicroTrap, Michrom Bioresources, Inc.) using a step elution of ammonium acetate in buffer A (50, 75, 150, 200, 300, 400, and 500mM NH_4OAc) to remove residue Coomassie blue dye.

LC-MS data acquisition and analysis: Peptides were separated with a 75 min, 2-80% acetonitrile gradient in 0.1% formic acid and one-dimensional liquid chromatography using an EASY n-LC UHPLC system (Thermo-Fisher Scientific) with a 2-cm Dionex Acclaim PepMap 100 (C18, 3 μm, 100Å) trap column (Dionex, Sunnyvale, CA), and a 15-cm Dionex Acclaim PepMap RSLC (C18, 2 μm, 100 Å) separating column (Dionex) and tandem mass spectrometry data generated by nanospray ionization into an LTQ Orbitrap ELITE mass spectrometer (Thermo-Fisher Scientific).

Data were acquired using the LTQ-Orbitrap ELITE mass spectrometer with an approach known as an Nth Order Double Play with electron transfer dissociation (ETD) Decision Tree method to exploit peptide fragmentation data acquisition by ETD and CID/HCD approaches (Swaney *et al.*, 2008). The acquired FTMS and ITMS data were analyzed using Proteome Discoverer (v1.3.0.339, Thermo-Fisher Scientific) and searched first using the UniprotKB mouse reference proteome (canonical and isoform sequence, version 01/25/2013) and subsequently for Rodentia for Arg-C digests assuming no modifications and for tryptic digests assuming carbamidomethylation of cysteine residues as a fixed modification and oxidation of methionine residues as a variable modification. A decoy database strategy was used to curtail the false discovery rate (decoy.pl (matrixscience.com)). All peptides spectra scoring higher by analysis against a reversed mouse database were eliminated from further consideration. Protein identification was accepted if it could be established at >95.0% probability and contained at least 2 or more unique peptides below the 1% false discovery rate.

Spectra were filtered by mass range (350-5000Da) total intensity threshold (0) and minimum peak counts (1). Scan event filters were used to define HCD and ETD spectra. For FT-only spectra were filtered with a S/N threshold of 1.5. All spectra were normalized and a Top N Peaks filter of 6 within a 100 Da mass window were used to simplify data submitted for analysis. Non-fragment filters were used to clip precursor spectra (+/−2 Da) around precursor masses, to remove charge reduced precursors (+/−1Da) and FT-precursor overtones (+/−0.5Da). For Mascot analysis of ITMS data a precursor mass tolerance of 50 ppm, a fragment mass tolerance of 1.2 Da and a peptide ion score cutoff of 10 were used to filter peptide assignments. For Arg-C and trypsin digests, dynamic modifications of C, H, and K were then selected for three acrolein adducts including H2C3 (38.02 Da), H4C3O1 (56.03 Da), H6C6O1 (94.04 Da), and five carnosine-acrolein adductions (Baba *et al.*, 2013) including C12H18N4O4 (+264.122 Da), C15H18N4O3 (+282.133 Da), C15H20N4O4 (+302.138 Da), C15H20N4O4 (+320.148 Da) and C15H22N4O5 (+338.159 Da). All other settings were similar to Mascot searches. Data were aggregated and used to make lists of high probability/high confidence peptide/protein assignments as shown. The resulting msf files from the searches were loaded into Scaffold v3.6.5 (proteomesoftware.com) and compared as individual experiments or aggregated as a MudPit experiment.

2.4. Histology, immunohistochemistry and immunofluorescence

Gross histology was determined in formalin-fixed, paraffin-embedded tissue sections (4 μm) stained with H&E, myeloperoxidase (MPO) or for apoptosis (TUNEL Apoptosis Kit, Chemicon, Milipore, Temecula, CA, USA) according to manufacturer's instructions.

Antibody against human GSTP1 (1:1500; Novocastra, Newcastle, UK) (Green *et al.*, 2005) was used with a Vector Elite or Envision Plus staining kit, respectively, using diaminobenzadine (DAB; Dako, Glostrup, Denmark) as chromagen. Using images representative of overall staining, the number of apoptosis- and MPO-positive cells was counted in a single, mid-left ventricular cross-section (i.e., # cells/LV section).

To assess selective GSTP expression, freshly isolated cardiomyocytes (Keith et al. 2009) were cultured overnight in laminin-coated chamber slides and media was changed after 16h (Keith *et al.*, 2009). Cardiomyocytes were fixed (4% PFA/PBS, pH=7.4, 10 min at room temperature), permeabilized (0.1% Triton X-100/PBS, 3 min at room temperature) and incubated for 15 min in 1% BSA/PBS. Cells were incubated with primary antibodies against GSTP (1:250, Proteintech, Chicago, IL) at 4°C for 6h. The cells were then incubated with an appropriate fluorescently-labeled secondary antibody (1:500, Alexa Fluor 488, Molecular Probes, Invitrogen, Carlsbad, CA) for 1h at room temperature. Slides were covered with DAPI containing *Slow Fade*® Gold antifade reagent (Molecular Probes, Invitrogen, Carlsbad, CA) and fluorescence was visualized on a Nikon A1 Confocal Microscope. GSTP-specific staining was discerned by using equivalent energy spectra for WT and GSTP-null cells using the NIS-Elements software (Nikon, Japan).

2.5. Data analysis

Data are mean ± SEM. Individual groups were compared using paired or unpaired Student's *t*-test or One Way ANOVA with Bonferroni post-hoc test where appropriate (SigmaStat, SPSS, Inc., Chicago, Il). Chi-square analysis was used to determine significance in survival experiments. $P<0.05$ was considered significant.

3. Results

3.1. Cardiac distribution of GSTP

Cardiac abundance of GSTP protein was examined by Western blotting GST activity and immunohistochemistry (**Fig. 1**). Western blotting showed abundant GSTP protein in lysates obtained from WT but not GSTP-null hearts (**Fig. 1A**). Similar levels of GSTA and GSTM proteins were present in WT and GSTP-null hearts (**Fig. 1A**). Sections of WT heart were immunopositive for GSTP in cardiomyocytes and smooth muscle layers of coronary blood vessels while hearts of GSTP-null mice were negative (**Fig. 1B**). GST conjugating activity was significantly less in hearts of GSTP-null compared with WT mice (**Fig. 1C**). In whole heart homogenates, total GST and GSTP-specific activities measured with substrates 1-chloro-2,4-dinitrobenzene (CDNB) and ethacrynic acid (EA), respectively, were significantly lower in GSTP-null than in WT mice, indicating that GSTP contributes approximately 40% of total cardiac GST activity. Moreover, isolated WT cardiomyocytes had specific cytoplasmic GSTP-immunofluorescence whereas GSTP staining was absent in GSTP-null cardiomyocytes (**Fig. 1D**).

3.2 Cyclophosphamide (CY) cardiotoxicity

Although 100 and 200 mg/kg CY did not affect CK·MB release, administration of 300 mg/kg CY led to a 2-fold increase in plasma CK levels 4h post-treatment in WT mice (**Fig.**

2A). Plasma CK·MB levels were strongly correlated with plasma CK levels ($r^2 = 0.96$; see Inset **Fig. 2A**) indicating that the heart was a likely (yet not sole) source of increased plasma CK. Notably, treatment of GSTP-null mice with a 300 mg/kg dose of CY led to a >20-fold increase in plasma CK levels (**Fig. 2A**). This result suggests that GSTP-null mice are profoundly more sensitive to CY-induced toxicity than WT mice.

To examine the selective effects of CY on cardiac injury, we measured cardiac function by echocardiography at 1h and 4h post-CY (300 mg/kg) in WT and GSTP-null mice (**Table 1**). CY modestly, yet significantly, altered cardiac dimensions and function in both WT and GSTP-null mice with most changes occurring at 1h, and then diminishing or resolving by 4h post-CY (**Table 1**). For example, CY significantly increased the velocity of circumferential fiber shortening (Vcf and Vcfc, i.e., the latter is corrected for heart rate) in GSTP-null, but not WT, hearts at 1h, an effect that was statistically insignificant (p=0.087) at 4h post-treatment (**Table 1**). In contrast, CY-induced a significant increase in fractional change in area (FAC; %) in both WT and GSTP-null at 1h post-CY that was a function of decreased end systolic area (ESA, mm^2) in both WT and null mice (**Table 1**). The effects of CY on ESA and FAC were absent in both WT and GSTP-null hearts at 4h post-treatment indicating this effect was reversible. This observation is consistent with clinical literature showing that high-dose CY associated cardiac toxicity is potentially reversible (Morandi *et al.*, 2001; Morandi *et al.*, 2005). Surprisingly, ejection fraction (EF) was slightly increased in WT mice at both 1h and 4h post-CY yet unaffected in GSTP-null hearts (p=0.053; 1h only; **Table 1**). Increased EF was likely due to decreased end systolic volume (ESV) at 1h (p=0.014) and 4h (p=0.062) in WT hearts, and ESV reflects more complete emptying of LV in WT hearts than in GSTP-null (p=0.10) mice. Ejection time (ET, a measure of aortic blood flow velocity) was significantly decreased in GSTP-null hearts only at 4h post-CY (**Table 1**). These data indicate that GSTP-null hearts were more sensitive to acute cardiac injury due to a rapid-onset and reversible form of altered contractility than that observed in WT mice.

To assess the dose-dependence of CY-induced cardiotoxicity, WT and GSTP-null mice were treated with lower doses of CY (100 and 200 mg/kg). CY treatment (200 mg/kg, 24h) also increased heart wet weight:body weight ratio significantly in GSTP-null but not in WT mice (**Fig. 2B**). CY induced a similar weight loss in WT and GSTP-null mice (WT: −2.65±0.30g, −9.40±1.06% bwt; GSTP-null: −2.68±0.27g, −9.28±1.01% bwt, n=5-6 mice). In contrast, CY-induced albumin extravasation (**Fig. 2C**) was significantly greater in GSTP-null mice (≈1.6-fold) when compared with WT mice (≈1.2-fold), indicating CY increased vascular permeability and plasma extravasation – an effect enhanced by GSTP depletion. Although, CY-induced cardiotoxicity was greater in magnitude in GSTP-null vs. WT mice, it was surprising that there was no change in the level of reduced glutathione (GSH) in either CY-treated WT or GSTP-null hearts at 4h post-treatment compared with matched control (WT: control, 25.7±3.9; +CY, 20.2±1.7; Null: control, 18.4±2.0; +CY, 20.6±2.2; n=4-6 mice). Normalization of GSH level to nmoles GSH per mg wet weight (**Fig. 2D**) also indicated that there was no statistically significant difference between WT and GSTP-null mice. Although GSH level was unchanged, treatment with CY for 4h led to a dose-dependent increase in the presence of the active form of caspase-3 in WT mice as analyzed by Western blot (**Fig. 2E**); similar results were observed in GSTP-null mice after CY treatment. Although no obvious

histopathological changes in myocardial structure (e.g., contraction band necrosis; data not shown) were observed, mid-left ventricular cross-sections had slightly increased apoptosis by TUNEL staining (**Fig. 2F**) and inflammation (MPO+ cells, **Suppl. Fig. S2**) in mice treated with CY (200 mg/kg), and these effects were similar in both WT and GSTP-null (although less MPO+ staining was in null mice) mice. Hemodynamically, CY decreased blood pressure and heart rate to a similar level in GSTP-null and WT mice at 4h post-CY (200 mg/kg) treatment (**Table 2**). Taken together, these results indicate that the differential cardiotoxicity of CY in GSTP-null mice is not a result of increased myocardial apoptosis or systemic hypotension.

3.3. CY-induced MAPK phosphorylation

Genomic deletion of *mGstP1/P2* constitutively activates JNK in bone marrow, liver and lung (Elsby *et al.*, 2003; Gate *et al.*, 2004), and increases CY-induced JNK and c-Jun activation in urinary bladder of GSTP-null mice compared with similarly-treated WT mice (Conklin *et al.*, 2009b). Although there was no evidence of constitutive JNK activation in hearts of GSTP-null mice, CY treatment led to a dose-dependent increase in phospho-JNK in both WT and GSTP-null mice (**Fig. 3A; see Suppl. Fig. S1** for full Western blot). No significant difference in the level of CY-induced JNK phosphorylation was found between GSTP-null and WT mice. In contrast, dose-dependent phosphorylation of c-Jun was observed only in GSTP-null mice (**Fig. 3B**). Similar to JNK, ERK phosphorylation was stimulated by CY to a significant degree in WT but not GSTP-null mice (**Fig. 3C**). CY treatment (100 or 300 mg/kg) increased phosphorylation of p38 in GSTP-null and WT mice, respectively (**Fig. 3D**). These observations indicate that deletion of GSTP increases the sensitivity of the heart to CY-induced c-Jun and p38 phosphorylation, but not CY-induced JNK or ERK phosphorylation, suggesting that selective pathways of MAPK signaling may be important in regulating the differential cardiotoxicity of CY in GSTP-null versus WT mice.

3.4. CY-induced formation and accumulation of protein-acrolein adducts

To examine specific GSTP-dependent changes in myocardial-acrolein reactivity in CY-treated mice, we examined changes in the myocardial abundance of protein-acrolein adducts (**Fig. 4; see Suppl. Fig. S2** for whole Western blot). Western blot analyses of these adducts revealed differences in adduct abundance between the control (saline) and CY (100, 200 and 300 mg/kg) treatment groups in WT (**Fig. 4A**) and GSTP-null mice (**Fig. 4B**). At 4h post-treatment, specific molecular mass (Mr) bands showed greater intensity in CY-treated mice compared with controls, and elevated levels of protein-acrolein adducts were found in GSTP-null mice when compared with WT mice. For example, CY (300 mg/kg) significantly increased the intensity of a protein band detected at ≈100 kDa in GSTP-null mice when compared with saline-treated control or lower dose CY-treated (100 mg/kg) GSTP-null mice (**Fig. 4B**). More importantly, at CY doses of 200 (≈1.4-fold) and 300 mg/kg (≈2-fold) the intensities of the band at ≈100 kDa were significantly higher in GSTP-null than in WT mice (compare **Fig. 4A** vs. **4B**; $^{\#}$ $p<0.05$ WT vs. GSTP-null). Similarly, the intensity of the band detected at ≈80 kDa was significantly greater (≈2.2 fold) in GSTP-null mice than in CY-treated WT (300 mg/kg) and in saline-treated GSTP-null mice. The density of other bands

(e.g. ≈250, ≈28 and ≈25 kDa) was not different between WT and GSTP-null mice; however, different patterns of protein-acrolein adduct abundance were observed. In GSTP-null mice the bands at ≈250 and ≈28 kDa were significantly increased after CY (200 or 300 mg/kg) compared with CY (100 mg/kg) or saline control, respectively, but were not increased in CY-treated WT mice. In contrast, a protein band at ≈25 kDa was significantly increased in WT hearts where only a marginal increase was observed in CY-treated GSTP-null hearts ($^{+}0.10>p>0.05$). Taken together, these results demonstrate that CY increases the abundance of protein-acrolein adducts in the heart and that the accumulation of several such adducts was greater in CY-treated GSTP-null than in CY-treated WT hearts.

Specific proteins likely modified by acrolein in CY-treated hearts were identified by mass spectrometry. For this, cardiac lysate of CY-treated mice was immunoprecipitated using protein-acrolein antibody and the precipitate was subjected to protein digestion and mass spectrometry. Following either Arg-C or trypsin digestion, we identified a small subset of precipitated proteins with high fidelity matches in the Mascot database (**Table 3**). Five of the top 20 proteospecific peptide matches were identified as kallikrein 1-related peptidases (MW 28-29 kDa), several of these had specific acrolein post-translational modifications (PTMs), and a major protein band at 28 M_r was present in Western blots of hearts from CY- (**Fig. 3**) and acrolein- (**Fig. 4**) treated mice. Serum albumin was also identified in the Mascot search (**Fig. 3; Table 3**). In addition, myoglobin and transgelin-2 were identified as cardiac proteins potentially modified by acrolein (**Table 3**). Because of the high abundance of non-cardiac proteins in the heart, these results indicate an increased vascular permeability in the CY-treated heart.

3.5. Acrolein Cardiotoxicity

Because GSTP is a multi-functional protein, it could protect the heart from CY toxicity by several potential mechanisms. However, because a major biochemical function of GSTP is to catalyze the conjugation of glutathione with electrophilic substrates such as acrolein (Berhane *et al.*, 1994), we hypothesized that the protective effects of GSTP relate to increased removal and detoxification of acrolein, which is a major toxic product of CY (Cox, 1979). To test this hypothesis, we examined whether GSTP regulates the cardio-toxic effects of acrolein by comparing acrolein toxicity in WT and GSTP-null mice.

At a dose of 1 mg/kg (ip) acrolein did not affect blood pressure or heart rate 1h post-treatment, but at 3 mg/kg a significant decrease in blood pressure was observed to the same extent in WT and GSTP-null mice without a change in heart rate (**Table 4**). In WT mice, these changes did not lead to an increase in heart wet weight:body weight ratio, although this ratio was significantly increased in GST-null mice (**Fig. 5A**). Moreover, treatment with acrolein (5 mg/kg; ip) resulted in significantly slowed ejection time (ET, **Fig. 5B**), which was more severe in GSTP-null than in WT hearts, although plasma CK levels were not significantly elevated in either WT (169±49 IU/L) or GSTP-null (111±33 IU/L) mice. Acrolein (5 mg/kg, po) treatment induced progressive and sustained hypoalbuminemia in both WT and in GSTP-null mice up to 24h post-acrolein (**Fig. 5C**), reflecting increased systemic vascular permeability. Taken together, these data indicate that acrolein causes systemic changes and sub-lethal myocardial injury in mice and that the absence of GSTP

exacerbates the cardiotoxic effects of acrolein. Treatment with a single dose of acrolein (5 mg/kg, po) did not result in significant mortality 24h after treatment in either WT or GSTP-null mice. However, treatment with acrolein at a dose of 10 mg/kg (ip or po) led to 14 or 21 % mortality in WT mice, respectively, that was significantly increased to 60 % in GSTP-null mice treated orally with acrolein. Treatment of GSTP-null mice by intraperitoneal injection of acrolein elevated mortality to 33 %. Seventy-five percent of WT mice died at a dose of 20 mg/kg acrolein (po) and none of GSTP-null mice survived (100 % mortality) this dose independent of the route of administration (ip or po; **Fig. 5D**). These observations suggest that GSTP-null mice are more sensitive to acrolein-induced lethality than WT mice.

To identify the GSTP dependence of acrolein cardiotoxicity in more detail, we examined systemic changes in GSH and TBARS levels, which are indicative of oxidative stress. No differences in tissue TBARS levels were detected in heart and liver, kidney, red blood cells, small intestine, and stomach at any time point between any of the treatment and control groups (data not shown). Measurements of GSH levels in tissues collected from acrolein-treated mice showed significant GSH depletion in the heart and stomach within 1h of treatment, and acrolein-induced GSH depletion in the heart was more severe in GSTP-null than in WT mice (**Table 5; Suppl. Fig. S4**). The changes in stomach GSH levels in WT and GSTP-null mice were similar (**Table 5**). No changes in liver GSH levels were observed. Time-dependent changes in plasma protein-acrolein adducts were detected in mice gavaged with acrolein (**Suppl. Fig. S3; Suppl. Table 1**). These results reinforce the view that GSTP plays a prominent role in regulating the selective cardiovascular toxicity of acrolein.

4. Discussion

The major finding of this study is that GSTP protects against the cardiotoxic effects of CY. Because GSTP metabolizes acrolein, the exacerbation of CY toxicity in GSTP-null mice is consistent with the notion that GSTP protects against CY cardiotoxicity by detoxifying acrolein generated during activation of the pro-drug. The GSTP-null hearts are more sensitive to CY-induced tissue injury as reflected by increased accumulation of proteins (cardiac and non-cardiac) adducted with acrolein (see **Table 3**), increased permeability and stress responses consistent with a view that GSTP mitigates CY toxicity by removing acrolein. These observations lend further support to the view that metabolic generation of acrolein is a significant cause of the cardiotoxic effects of CY treatment. Overall, these findings have wide implications in preventing and minimizing adverse cardiac outcomes of high dose CY chemotherapy.

Clinical studies show that high-dose CY therapy is often associated with congestive heart failure, which has been linked to extensive endothelial damage and frank myocyte death. These changes are frequently associated with life-threatening arrhythmias. Patients with fulminant cardiotoxicity following CY therapy show myocardial hemorrhage, pericardial effusion and fibrinous pericarditis (Katayama *et al.*, 2009). Even in the absence of clinical heart failure, some patients show increased troponin levels in the blood after CY therapy and a decrease in early diastolic Doppler velocities (Em) during individual cycles of chemotherapy indicating deterioration of left ventricular diastolic function (Zver *et al.*, 2008). While we did not measure electrical activity, several of the other clinical features of

CY toxicity were recapitulated in our model, which showed increased myocyte injury (increased plasma CK·MB), fluid extravasation/edema (increased heart-to-body weight ratio and albumin levels) and circumferential hypercontractility. Importantly, these manifestations of CY toxicity were exaggerated in hearts of GSTP-null mice. These data support the view that the absence of GSTP increases necrotic cell death in the heart. Although CY treatment increased apoptosis (**Fig. 2E&F**) that conceivably contributed to overall myocardial injury, this form of cell death was not affected by GSTP status. Necrosis in CY-treated hearts could result from hypercontracture (e.g., calcium overload) and this possibility is supported by echocardiographic data indicating a slightly greater cardiac contractility stimulated by CY (1h) in GSTP-null mice (see Table 3). While both EF and FAC reflect changes in LV chamber dimension and are altered similarly in WT and GSTP-null mice, Vcf (velocity), a measure of the rate of contraction and a more sensitive index of cardiotoxicity (Syed *et al.*, 2005), was uniquely and robustly increased in GSTP-null but not in WT mice. Sustained hypercontractility likely reflects increased intracellular calcium and also portends enhanced cardiac injury and CK·MB leak due to compromised sarcolemma integrity, however, these contractile changes are modest and did not reach levels constituting a definition of left ventricular dysfunction (e.g., EF<45%). A similar acute cardiotoxicity profile with modest diastolic (contractile) dysfunction with more prominent interstitial edema is observed in humans (Morandi *et al.*, 2001).

Although GSTP could potentially regulate CY toxicity by altering its metabolism, our results suggest that GSTP-mediated cardioprotection is independent of the rate of CY activation (i.e., P450-dependent metabolism), which if higher in null mice would lead to greater levels of acrolein (and injury) in GSTP-null mice. Both CY and acrolein induce systemic hypotension to a similar level in both WT and GSTP-null mice indicating that CY is activated similarly in GSTP-null and WT mice. This is consistent with our previous finding that P450 activation of CY is similar in liver microsomes of WT and GSTP-null mice (Pope *et al.*, 2008). Moreover, it is unlikely that GSTP regulates CY toxicity by altering its conversion to phosphoramide mustard, but rather by metabolizing acrolein generated from CY.

A causal role of acrolein in mediating CY toxicity is consistent with the view that metabolism of CY could generate lethal levels of this cytotoxic aldehyde. Approximately 70% of a CY dose is activated by hepatic P450s (Sladek, 1994; Yu *et al.*, 1999) and acrolein (F.W. 56) is 20% of the molecular mass of CY (F.W. 279.1), so a CY dose of 300 mg/kg body weight produces an acrolein equivalent dose of ~42 mg/kg body weight. This acrolein equivalent dose is twice the lethal acrolein dose in mice and several times the acrolein dose used in the present study. Moreover, this CY dose compares favorably with the LC_{10} of CY (i.e., 1391 mg/m^2 = 464 mg/kg) in mice, which would result in even a greater level of acrolein (≈65 mg/kg bwt)(Friedman *et al.*, 1990). The 300 mg/kg dose of CY used in mice is equivalent to approximately 140 mg/kg body weight dose in humans (Friedman *et al.*, 1990), which is well within the range of high dose CY used clinically. Thus, CY treatment is potentially capable of generating acrolein in quantities sufficient to precipitate cell death. Although the mechanism of acrolein-induced cardiotoxicity was not studied in detail here, our previous studies have shown that acute acrolein exposure results in reversible ventricular

dilation and depressed cardiac myocyte contractility (Luo *et al.*, 2007), whereas chronic exposures lead to LV dilation, contractile dysfunction and impaired relaxation (Ismahil *et al.*, 2011). These phenotypic changes resemble CY-induced myocardial changes both in mice (**Fig. 2**) and humans (Morandi *et al.*, 2005), which supports the view that acrolein mediates CY-induced cardiotoxicity.

An obligatory role of acrolein in mediating CY toxicity is further supported by the observations that co-administration of thiol-containing nucleophiles such as MESNA or N-acetylcysteine protects against CY toxicity and conversely depletion of GSH by buthionine-SR-sulfoximine (BSO) increases the cardiotoxic effects of CY (Friedman *et al.*, 1990). Acrolein reacts avidly with GSH (Berhane *et al.*, 1994) and the acrolein-glutathione adduct is actively extruded from the cell (Awasthi *et al.*, 2003) and increasing cellular thiols mitigates acrolein toxicity (Batista *et al.*, 2007). Therefore, the protective effects of MESNA and other thiols against CY toxicity are consistent with a causative role of acrolein in CY toxicity. Nevertheless, a direct role of this aldehyde in mediating CY-toxicity is difficult to assess and has not been convincingly demonstrated before. In this regard, the present data showing that CY cardiotoxicity is exacerbated by deleting the acrolein-metabolizing enzyme GSTP provide a line of evidence in support of the view that acrolein plays an important role in CY toxicity. However, whether acrolein directly causes myocardial injury or merely enhances the toxicity of phosphoramide mustard by depleting glutathione remains unclear (Friedman *et al.*, 1990). Our measurements indicate that the severity of CY-induced GSH depletion was not increased in GSTP-null hearts, suggesting that the increase in CY-induced toxicity in GSTP-null hearts may be independent of GSH depletion and related more so to direct toxic effects of acrolein (e.g., endothelial permeability), protein-acrolein adducts (Luo *et al.*, 2007) or other mechanisms regulated by GSTP.

We found that protein-acrolein adducts were increased in the heart upon treatment with either acrolein or CY. Therefore, to shed light on potential contribution of such protein modification, we used an unbiased approach to identify protein targets that led to the identification of a small set of high fidelity matches by mass spectrometry (**Table 3**). In particular, the presence of acrolein-modified kallikrein 1-related peptidases, a member of a large gene family cluster on human chromosome 19, was surprising because it is not a cardiac enzyme (Olsson and Lundwall, 2002; Parikh *et al.*, 2011), and thus, its presence in the heart may be indicative of deposition from extracellular sites. The kallikrein 1- and 3-related peptidases are recognized both as a potential ‘radiation biodosimeter’ (Sharma and Moulder, 2013) and as a ‘co-marker’ (along with PSA) of prostate cancer (Parikh *et al.*, 2011), respectively, indicating that kallikrein 1-related peptidase potentially could be a new marker of CY-induced prostate or systemic toxicity. Because modified albumin also was increased in CY-treated heart, we speculate that the presence of extra-cardiac proteins in the heart may result from increased vascular permeability leading to edema and an increase in the heart weight/bwt ratio (**Fig. 2**). Acrolein modification of myoglobin in CY-treated hearts also may be significant. Several previous studies have shown that heme containing proteins such as hemoglobin and myoglobin are readily modified by α,β-unsaturated aldehydes and that structural changes induced by such modification decrease reduction of MetMb to deoxyMb and increases its catalytic activity as a lipid pro-oxidant (Faustman *et al.*, 1999;

Lynch and Faustman, 2000; Alderton *et al.*, 2003). Thus, modification of myoglobin in the heart by acrolein may be a significant mechanism underlying increased oxidative stress and cell injury induced by CY therapy. Similarly, modification of the actin-associated protein transgelin also may be a contributing factor to contractile dysfunction of CY-treated hearts. Further research is required to determine how modification of these individual proteins by acrolein contributes to the cardiotoxicity associated with CY treatment.

Although GSTP plays a major role in acrolein detoxification, it is a multi-functional enzyme (Adler *et al.*, 1999) and may regulate CY-toxicity independent of acrolein metabolism. Recent work from our laboratory has shown that GSTP mediates glutathiolation of sulfenic acid-modified proteins and thereby prevents subsequent irreversible protein oxidation to sulfinic or sulfonic acids (Wetzelberger *et al.*, 2010). In addition it has also been shown that GSTP protects against stress and cytokine signaling by regulating MAPK activation via protein-protein interactions as demonstrated for GSTP-JNK and GSTP-TRAF2 signaling (Xue *et al.*, 2005; Wu *et al.*, 2006). Notably, genetic deletion of murine *Gstp1/p2* constitutively activates JNK/c-Jun in bone marrow, liver and lung (Elsby *et al.*, 2003; Gate *et al.*, 2004) but not in the urinary bladder (Pope *et al.*, 2008). However, in the present study, we did not observe constitutively phosphorylated JNK and c-Jun in the GSTP-null heart, yet CY induced greater c-Jun activation in GSTP-null heart compared with WT (Fig. 3B), supporting the general model that GSTP prevents JNK-mediated phosphorylation of c-Jun (Adler and Pincus, 2004). Furthermore, hearts of GSTP-null mice were more sensitive to CY-induced p38 phosphorylation than WT hearts (Fig. 3D), and phospho-p38 can upregulate inflammatory genes and compromise sarcolemma integrity following ischemia-reperfusion (Maulik, 2005; Tenhunen *et al.*, 2006). Surprisingly, we did not observe greater inflammation (measured as MPO^+ cells) in CY-treated GSTP-null than WT hearts (see **Suppl. Fig. S2C**); an effect nonetheless prevented by MESNA pretreatment (data not shown). In any case, because these signaling events are also activated by acrolein (Haberzettl *et al.*, 2009), it seems likely that increased stress signaling in the CY-treated GSTP-null heart may be due to increased acrolein presence in the hearts of GSTP-null mice lacking appropriate metabolism and detoxification of acrolein.

The role of GSTP in preventing CY toxicity demonstrated here has broad clinical implications. Our findings suggest that myocardial GSTP levels are likely to be key determinants of CY cardiotoxicity. GSTP is a highly-regulated enzyme that is readily induced by different environmental factors, diet constituents such as garlic organosulfur compounds, coffee and chemopreventive agents such as selenocysteine conjugates (Steinkellner *et al.*, 2005; Lii *et al.*, 2010). Therefore, GSTP induction by such agents could attenuate CY toxicity, and conversely, disturbed metabolic states such as obesity, which are associated with down-regulation of GSTP (Conklin *et al.*, 2010; Kirpich *et al.*, 2011), could enhance the cardiotoxicity of CY treatment. Moreover, the human GSTP gene is polymorphic and *GSTP1* polymorphic variants (l104V, A113V) differ in their catalytic efficiency towards acrolein (Pal *et al.*, 2000). Thus, it is likely that polymorphic variations in GSTP could affect CY toxicity, and although the role of GSTP polymorphisms in regulating the cardiotoxic effects of CY has not been studied, it has been reported that a single nucleotide polymorphism (SNP; A313G, I104V) in *GSTP1* gene increases the relative risk

of congestive heart failure in adults who were treated with anthracycline chemotherapy for childhood leukemia (Aplenc *et al.*, 2006). The polymorphism associated with the highest risk (A313G) codes for the I104V residue that influences GSTP conjugation activity and in combination with a second polymorphic site, C341T → A113V, results in an allelic switch (i.e., IA to VV) that significantly alters GSTP activity toward specific substrates, including acrolein (Pal *et al.*, 2000). Therefore, additional pharmacogenomic studies are required to determine whether GSTP polymorphisms also increase cardiac sensitivity to CY and whether the GSTP genotype could be used to identify patients that might be more sensitive to high-dose CY chemotherapy (Ekhart *et al.*, 2008; Sharda *et al.*, 2008).

Supplementary Material

Refer to Web version on PubMed Central for supplementary material.

Acknowledgements

This work was supported by American Health Assistance Fund/National Heart Foundation grant #2007-202 (DJC) and NIH grants: P20 GM103492-06 (AB), ES11860 (AB), HL89380 (DJC), HL59378 (SDP), a Veterans Affairs Merit Award (SDP), and T35 ES014559 (JDW, RAP). We thank B. Bishop, K. Brittain, E. Cardwell, L. Guo, L. Haberzettl, J. Marshall, D. Mosley, E. Steinmetz, L. Stephens, A. Tang, E. Werkman and D. Young for expert technical assistance. We thank Dr. S.P. Jones, Univ. of Louisville, for his invaluable input and assistance with confocal microscopy. We thank Drs. C. Henderson and R. Wolf, University of Dundee, for donation of breeding pairs of GSTP1/P2 wild-type and null mice.

Glossary

CY	cyclophosphamide
GST	glutathione S-transferase

References

Adler V, Pincus MR. Effector peptides from glutathione-S-transferase-pi affect the activation of jun by jun-N-terminal kinase. Ann.Clin.Lab Sci. 2004; 34:35–46. [PubMed: 15038666]

Adler V, Yin Z, Fuchs SY, Benezra M, Rosario L, Tew KD, Pincus MR, Sardana M, Henderson CJ, Wolf CR, Davis RJ, Ronai Z. Regulation of JNK signaling by GSTp. EMBO J. 1999; 18:1321–1334. [PubMed: 10064598]

Al-Rawithi S, El-Yazigi A, Ernst P, Al-Fiar F, Nicholls PJ. Urinary excretion and pharmacokinetics of acrolein and its parent drug cyclophosphamide in bone marrow transplant patients. Bone Marrow Transplant. 1998; 22:485–490. [PubMed: 9733272]

Alderton AL, Faustman C, Liebler DC, Hill DW. Induction of redox instability of bovine myoglobin by adduction with 4-hydroxy-2-nonenal. Biochemistry. 2003; 42:4398–4405. [PubMed: 12693935]

Aplenc R, Blanco J, Leisenring W, Davies S, Relling M, Robison L, Sklar C, Stovall M, Bhatia S. Polymorphisms in candidate genes in patients with congestive heart failure (CHF) after childhood cancer: A Report from the Childhood Cancer Survivor Study (CCSS). American Society of Clinical Oncology. 2006

Awasthi S, Singhal SS, Sharma R, Zimniak P, Awasthi YC. Transport of glutathione conjugates and chemotherapeutic drugs by RLIP76 (RALBP1): a novel link between G-protein and tyrosine kinase signaling and drug resistance. Int.J.Cancer. 2003; 106:635–646. [PubMed: 12866021]

Baba SP, Hoetker JD, Merchant M, Klein JB, Cai J, Barski OA, Conklin DJ, Bhatnagar A. Role of aldose reductase in the metabolism and detoxification of carnosine-acrolein conjugates. J Biol Chem. 2013; 288:28163–28179. [PubMed: 23928303]

Batista CK, Mota JM, Souza ML, Leitao BT, Souza MH, Brito GA, Cunha FQ, Ribeiro RA. Amifostine and glutathione prevent ifosfamide- and acrolein-induced hemorrhagic cystitis. Cancer Chemother.Pharmacol. 2007; 59:71–77. [PubMed: 16708234]

Berhane K, Widersten M, Engstrom A, Kozarich JW, Mannervik B. Detoxication of base propenals and other alpha, beta-unsaturated aldehyde products of radical reactions and lipid peroxidation by human glutathione transferases. Proc.Natl.Acad.Sci.U.S.A. 1994; 91:1480–1484. [PubMed: 8108434]

Biagini RE, Toraason MA, Lynch DW, Winston GW. Inhibition of rat heart mitochondrial electron transport in vitro: implications for the cardiotoxic action of allylamine or its primary metabolite, acrolein. Toxicology. 1990; 62:95–106. [PubMed: 2343460]

Bryant BM, Jarman M, Ford HT, Smith IE. Prevention of isophosphamide-induced urothelial toxicity with 2-mercaptoethane sulphonate sodium (mesnum) in patients with advanced carcinoma. Lancet. 1980; 2:657–659. [PubMed: 6106781]

Conklin DJ, Boyce CL, Trent MB, Boor PJ. Amine metabolism: a novel path to coronary artery vasospasm. Toxicology and Applied Pharmacology. 2001; 175:149–159. [PubMed: 11543647]

Conklin DJ, Haberzettl P, Bertke M, Bhatnagar A. Role of glutathione S-transferase P (GSTP) in high fat diet-induced obesity: Dissociation of endothelial dysfunction from insulin resistance. Circulation. 2010; 122:A17917.

Conklin DJ, Haberzettl P, Lesgards JF, Prough RA, Srivastava S, Bhatnagar A. Increased sensitivity of glutathione S-transferase P-null mice to cyclophosphamide-induced urinary bladder toxicity. J Pharmacol Exp Ther. 2009a; 331:456–469. [PubMed: 19696094]

Conklin DJ, Haberzettl P, Prough RA, Bhatnagar A. Glutathione-S- transferase P protects against endothelial dysfunction induced by exposure to tobacco smoke. Am.J.Physiol Heart Circ.Physiol. 2009b; 296:H1586–H1597. [PubMed: 19270193]

Cox PJ. Cyclophosphamide cystitis--identification of acrolein as the causative agent. Biochem.Pharmacol. 1979; 28:2045–2049. [PubMed: 475846]

Drimal J, Zurova-Nedelcevova J, Knezl V, Sotnikova R, Navarova J. Cardiovascular toxicity of the first line cancer chemotherapeutic agents: doxorubicin, cyclophosphamide, streptozotocin and bevacizumab. Neuro.Endocrinol.Lett. 2006; 27(Suppl 2):176–179. [PubMed: 17159809]

Ekhart C, Rodenhuis S, Smits PH, Beijnen JH, Huitema AD. Relations between polymorphisms in drug-metabolising enzymes and toxicity of chemotherapy with cyclophosphamide, thiotepa and carboplatin. Pharmacogenet.Genomics. 2008; 18:1009–1015. [PubMed: 18854779]

Elsby R, Kitteringham NR, Goldring CE, Lovatt CA, Chamberlain M, Henderson CJ, Wolf CR, Park BK. Increased constitutive c-Jun N-terminal kinase signaling in mice lacking glutathione S-transferase Pi. Journal of Biological Chemistry. 2003; 278:22243–22249. [PubMed: 12646564]

Faustman C, Liebler DC, McClure TD, Sun Q. alpha,beta- unsaturated aldehydes accelerate oxymyoglobin oxidation. J Agric Food Chem. 1999; 47:3140–3144. [PubMed: 10552621]

Freireich EJ. Who took the clinical out of clinical research?--Mouse versus man: seventh David A Karnofsky Memorial Lecture--1976. Clin Cancer Res. 1997; 3:2711–2722. [PubMed: 10068279]

Friedman HS, Colvin OM, Aisaka K, Popp J, Bossen EH, Reimer KA, Powell JB, Hilton J, Gross SS, Levi R, et al. Glutathione protects cardiac and skeletal muscle from cyclophosphamide-induced toxicity. Cancer Res. 1990; 50:2455–2462. [PubMed: 2317829]

Gate L, Majumdar RS, Lunk A, Tew KD. Increased myeloproliferation in glutathione S-transferase pi-deficient mice is associated with a deregulation of JNK and Janus kinase/STAT pathways. Journal of Biological Chemistry. 2004; 279:8608–8616. [PubMed: 14684749]

Gil-Ortega I, Carlos Kaski J. [Diabetic miocardiopathy]. Med Clin (Barc). 2006; 127:584–594. [PubMed: 17145017]

Giraud B, Hebert G, Deroussent A, Veal GJ, Vassal G, Paci A. Oxazaphosphorines: new therapeutic strategies for an old class of drugs. Expert Opin Drug Metab Toxicol. 2010; 6:919–938. [PubMed: 20446865]

Green N, Weech M, Walters E. Localization and characterization of glutathione-s-transferase isozymes alpha, mu, and pi within the mouse vomeronasal organ. Neurosci.Lett. 2005; 375:198–202. [PubMed: 15694260]

Haberzettl P, Vladykovskaya E, Srivastava S, Bhatnagar A. Role of endoplasmic reticulum stress in acrolein-induced endothelial activation. Toxicol Appl Pharmacol. 2009; 234:14–24. [PubMed: 18951912]

Habig WH, Pabst MJ, Jakoby WB. Glutathione S-transferases. The first enzymatic step in mercapturic acid formation. Journal of Biological Chemistry. 1974; 249:7130–7139. [PubMed: 4436300]

Henderson CJ, Smith AG, Ure J, Brown K, Bacon EJ, Wolf CR. Increased skin tumorigenesis in mice lacking pi class glutathione S-transferases. Proc.Natl.Acad.Sci.U.S.A. 1998; 95:5275–5280. [PubMed: 9560266]

Ismahil MA, Hamid T, Haberzettl P, Gu Y, Chandrasekar B, Srivastava S, Bhatnagar A, Prabhu SD. Chronic oral exposure to the aldehyde pollutant acrolein induces dilated cardiomyopathy. Am J Physiol Heart Circ Physiol. 2011; 301:H2050–2060. [PubMed: 21908791]

Jensen, ON.; Shevchenko, A.; Mann, M. Protein analysis by mass spectrometry.. In: Creighton, TE., editor. Protein Structure. Oxford University Press; Oxford: 1997.

Katayama M, Imai Y, Hashimoto H, Kurata M, Nagai K, Tamita K, Morioka S, Furukawa Y. Fulminant fatal cardiotoxicity following cyclophosphamide therapy. J Cardiol. 2009; 54:330–334. [PubMed: 19782276]

Keith RJ, Haberzettl P, Vladykovskaya E, Hill BG, Kaiserova K, Srivastava S, Barski O, Bhatnagar A. Aldose reductase decreases endoplasmic reticulum stress in ischemic hearts. Chem Biol Interact. 2009; 178:242–249. [PubMed: 19041636]

Kirpich IA, Gobejishvili LN, Bon Homme M, Waigel S, Cave M, Arteel G, Barve SS, McClain CJ, Deaciuc IV. Integrated hepatic transcriptome and proteome analysis of mice with high-fat diet-induced nonalcoholic fatty liver disease. J Nutr Biochem. 2011; 22:38–45. [PubMed: 20303728]

Kuittinen T, Husso-Saastamoinen M, Sipola P, Vuolteenaho O, Ala-Kopsala M, Nousiainen T, Jantunen E, Hartikainen J. Very acute cardiac toxicity during BEAC chemotherapy in non-Hodgkin's lymphoma patients undergoing autologous stem cell transplantation. Bone Marrow Transplant. 2005; 36:1077–1082. [PubMed: 16247436]

Levine LA, Richie JP. Urological complications of cyclophosphamide. J.Urol. 1989; 141:1063–1069. [PubMed: 2651710]

Lii CK, Liu KL, Cheng YP, Lin AH, Chen HW, Tsai CW. Sulforaphane and alpha-lipoic acid upregulate the expression of the pi class of glutathione S-transferase through c-jun and Nrf2 activation. J Nutr. 2010; 140:885–892. [PubMed: 20237067]

Low JE, Borch RF, Sladek NE. Conversion of 4-hydroperoxycyclophosphamide and 4-hydroxycyclophosphamide to phosphoramide mustard and acrolein mediated by bifunctional catalysis. Cancer Res. 1982; 42:830–837. [PubMed: 7059981]

Ludeman SM. The chemistry of the metabolites of cyclophosphamide. Curr Pharm Des. 1999; 5:627–643. [PubMed: 10469895]

Luo J, Hill BG, Gu Y, Cai J, Srivastava S, Bhatnagar A, Prabhu SD. Mechanisms of acrolein-induced myocardial dysfunction: implications for environmental and endogenous aldehyde exposure. Am.J.Physiol Heart Circ.Physiol. 2007; 293:H3673–H3684. [PubMed: 17921335]

Lynch MP, Faustman C. Effect of aldehyde lipid oxidation products on myoglobin. J Agric Food Chem. 2000; 48:600–604. [PubMed: 10725121]

Maulik N. Effect of p38 MAP kinase on cellular events during ischemia and reperfusion: possible therapy. Am J Physiol Heart Circ Physiol. 2005; 289:H2302–2303. [PubMed: 16284105]

Morandi P, Ruffini PA, Benvenuto GM, La Vecchia L, Mezzena G, Raimondi R. Serum cardiac troponin I levels and ECG/Echo monitoring in breast cancer patients undergoing high-dose (7 g/m(2)) cyclophosphamide. Bone Marrow Transplant. 2001; 28:277–282. [PubMed: 11535996]

Morandi P, Ruffini PA, Benvenuto GM, Raimondi R, Fosser V. Cardiac toxicity of high-dose chemotherapy. Bone Marrow Transplant. 2005; 35:323–334. [PubMed: 15543194]

Motoki N, Shimizu T, Akazawa Y, Saito S, Tanaka M, Yanagisawa R, Motoki H, Nakazawa Y, Sakashita K, Iwasaki Y, Shiohara M, Koike K. Increased pretransplant QT dispersion as a risk factor for the development of cardiac complications during and after preparative conditioning for pediatric allogeneic hematopoietic stem cell transplantation. Pediatr Transplant. 2010; 14:986–992. [PubMed: 21108706]

Olsson AY, Lundwall A. Organization and evolution of the glandular kallikrein locus in Mus musculus. Biochem Biophys Res Commun. 2002; 299:305–311. [PubMed: 12437987]

Pal A, Hu X, Zimniak P, Singh SV. Catalytic efficiencies of allelic variants of human glutathione S-transferase Pi in the glutathione conjugation of alpha, beta-unsaturated aldehydes. Cancer Lett. 2000; 154:39–43. [PubMed: 10799737]

Parikh H, Wang Z, Pettigrew KA, Jia J, Daugherty S, Yeager M, Jacobs KB, Hutchinson A, Burdett L, Cullen M, Qi L, Boland J, Collins I, Albert TJ, Vatten LJ, Hveem K, Njolstad I, Cancel-Tassin G, Cussenot O, Valeri A, Virtamo J, Thun MJ, Feigelson HS, Diver WR, Chatterjee N, Thomas G, Albanes D, Chanock SJ, Hunter DJ, Hoover R, Hayes RB, Berndt SI, Sampson J, Amundadottir L. Fine mapping the KLK3 locus on chromosome 19q13.33 associated with prostate cancer susceptibility and PSA levels. Hum Genet. 2011; 129:675–685. [PubMed: 21318478]

Perini P, Calabrese M, Rinaldi L, Gallo P. The safety profile of cyclophosphamide in multiple sclerosis therapy. Expert.Opin.Drug Saf. 2007; 6:183–190. [PubMed: 17367264]

Pope CA 3rd, Renlund DG, Kfoury AG, May HT, Horne BD. Relation of heart failure hospitalization to exposure to fine particulate air pollution. Am J Cardiol. 2008; 102:1230–1234. [PubMed: 18940298]

Roberts JC, Francetic DJ, Zera RT. Chemoprotection against cyclophosphamide-induced urotoxicity: comparison of nine thiol protective agents. Anticancer Res. 1994; 14:389–395. [PubMed: 8017838]

Senkus E, Jassem J. Cardiovascular effects of systemic cancer treatment. Cancer Treat Rev. 2011; 37:300–311. [PubMed: 21126826]

Sharda SV, Gulati S, Tripathi G, Jafar T, Kumar A, Sharma RK, Agrawal S. Do glutathione-S-transferase polymorphisms influence response to intravenous cyclophosphamide therapy in idiopathic nephrotic syndrome? Pediatr.Nephrol. 2008; 23:2001–2006. [PubMed: 18594869]

Sharma M, Moulder JE. The urine proteome as a radiation biodosimeter. Adv Exp Med Biol. 2013; 990:87–100. [PubMed: 23378004]

Shepherd JD, Pringle LE, Barnett MJ, Klingemann HG, Reece DE, Phillips GL. Mesna versus hyperhydration for the prevention of cyclophosphamide-induced hemorrhagic cystitis in bone marrow transplantation. J.Clin.Oncol. 1991; 9:2016–2020. [PubMed: 1941060]

Sklar JL, Anderson PG, Boor PJ. Allylamine and acrolein toxicity in perfused rat hearts. Toxicology and Applied Pharmacology. 1991; 107:535–544. [PubMed: 2000639]

Sladek, NE. Metabolism and pharmacokinetic behavior of cyclophosphamide and related oxazaphosphorines. 1994. p. 79-156.

Srivastava S, Chandrasekar B, Bhatnagar A, Prabhu SD. Lipid peroxidation-derived aldehydes and oxidative stress in the failing heart: role of aldose reductase. Am.J.Physiol Heart Circ.Physiol. 2002; 283:H2612–H2619. [PubMed: 12388223]

Steinkellner H, Hoelzl C, Uhl M, Cavin C, Haidinger G, Gsur A, Schmid R, Kundi M, Bichler J, Knasmuller S. Coffee consumption induces GSTP in plasma and protects lymphocytes against (+/−)-anti-benzo[a]pyrene-7,8-dihydrodiol-9,10-epoxide induced DNA-damage: results of controlled human intervention trials. Mutation Research. 2005; 591:264–275. [PubMed: 16099480]

Swaney DL, McAlister GC, Coon JJ. Decision tree-driven tandem mass spectrometry for shotgun proteomics. Nat Methods. 2008; 5:959–964. [PubMed: 18931669]

Syed F, Diwan A, Hahn HS. Murine echocardiography: a practical approach for phenotyping genetically manipulated and surgically modeled mice. J Am Soc Echocardiogr. 2005; 18:982–990. [PubMed: 16153531]

Takamoto S, Sakura N, Namera A, Yashiki M. Monitoring of urinary acrolein concentration in patients receiving cyclophosphamide and ifosphamide. J Chromatogr B Analyt Technol Biomed Life Sci. 2004; 806:59–63.

Tenhunen O, Rysa J, Ilves M, Soini Y, Ruskoaho H, Leskinen H. Identification of cell cycle regulatory and inflammatory genes as predominant targets of p38 mitogen-activated protein kinase in the heart. Circ Res. 2006; 99:485–493. [PubMed: 16873723]

Toraason M, Luken ME, Breitenstein M, Krueger JA, Biagini RE. Comparative toxicity of allylamine and acrolein in cultured myocytes and fibroblasts from neonatal rat heart. Toxicology. 1989; 56:107–117. [PubMed: 2728003]

Vladykovskaya E, Sithu SD, Haberzettl P, Wickramasinghe NS, Merchant ML, Hill BG, McCracken J, Agarwal A, Dougherty S, Gordon SA, Schuschke DA, Barski OA, O'Toole T, D'Souza SE, Bhatnagar A, Srivastava S. Lipid peroxidation product 4-hydroxy-trans-2-nonenal causes endothelial activation by inducing endoplasmic reticulum stress. J Biol Chem. 2012; 287:11398–11409. [PubMed: 22228760]

Wetzelberger K, Baba SP, Thirunavukkarasu M, Ho YS, Maulik N, Barski OA, Conklin DJ, Bhatnagar A. Postischemic deactivation of cardiac aldose reductase: role of glutathione S-transferase P and glutaredoxin in regeneration of reduced thiols from sulfenic acids. J Biol Chem. 2010; 285:26135–26148. [PubMed: 20538586]

Worth L, Tran H, Petropoulos D, Culbert S, Mullen C, Roberts W, Przepiorka D, Chan K. Hematopoietic stem cell transplantation for childhood myeloid malignancies after high-dose thiotepa, busulfan and cyclophosphamide. Bone Marrow Transplant. 1999; 24:947–952. [PubMed: 10556952]

Wu Y, Fan Y, Xue B, Luo L, Shen J, Zhang S, Jiang Y, Yin Z. Human glutathione S-transferase P1-1 interacts with TRAF2 and regulates TRAF2-ASK1 signals. Oncogene. 2006; 25:5787–5800. [PubMed: 16636664]

Xue B, Wu Y, Yin Z, Zhang H, Sun S, Yi T, Luo L. Regulation of lipopolysaccharide-induced inflammatory response by glutathione S-transferase P1 in RAW264.7 cells. FEBS Lett. 2005; 579:4081–4087. [PubMed: 16023107]

Yu LJ, Drewes P, Gustafsson K, Brain EG, Hecht JE, Waxman DJ. In vivo modulation of alternative pathways of P-450-catalyzed cyclophosphamide metabolism: impact on pharmacokinetics and antitumor activity. J.Pharmacol.Exp.Ther. 1999; 288:928–937. [PubMed: 10027828]

Zver S, Zadnik V, Bunc M, Rogel P, Cernelc P, Kozelj M. Cardiac toxicity of high-dose cyclophosphamide in patients with multiple myeloma undergoing autologous hematopoietic stem cell transplantation. Int J Hematol. 2007; 85:408–414. [PubMed: 17562616]

Zver S, Zadnik V, Cernelc P, Kozelj M. Cardiac toxicity of high-dose cyclophosphamide and melphalan in patients with multiple myeloma treated with tandem autologous hematopoietic stem cell transplantation. Int J Hematol. 2008; 88:227–236. [PubMed: 18548196]

Highlights

- Acute cardiotoxicity of cyclophosphamide (CY) is exacerbated in GSTP-null mice
- CY altered cardiac contractility, vascular leak and protein-acrolein adducts
- Cardiotoxicity of CY is recapitulated by acrolein only exposure
- Acrolein-induced cardiotoxicity and mortality is enhanced in male GSTP-null mice

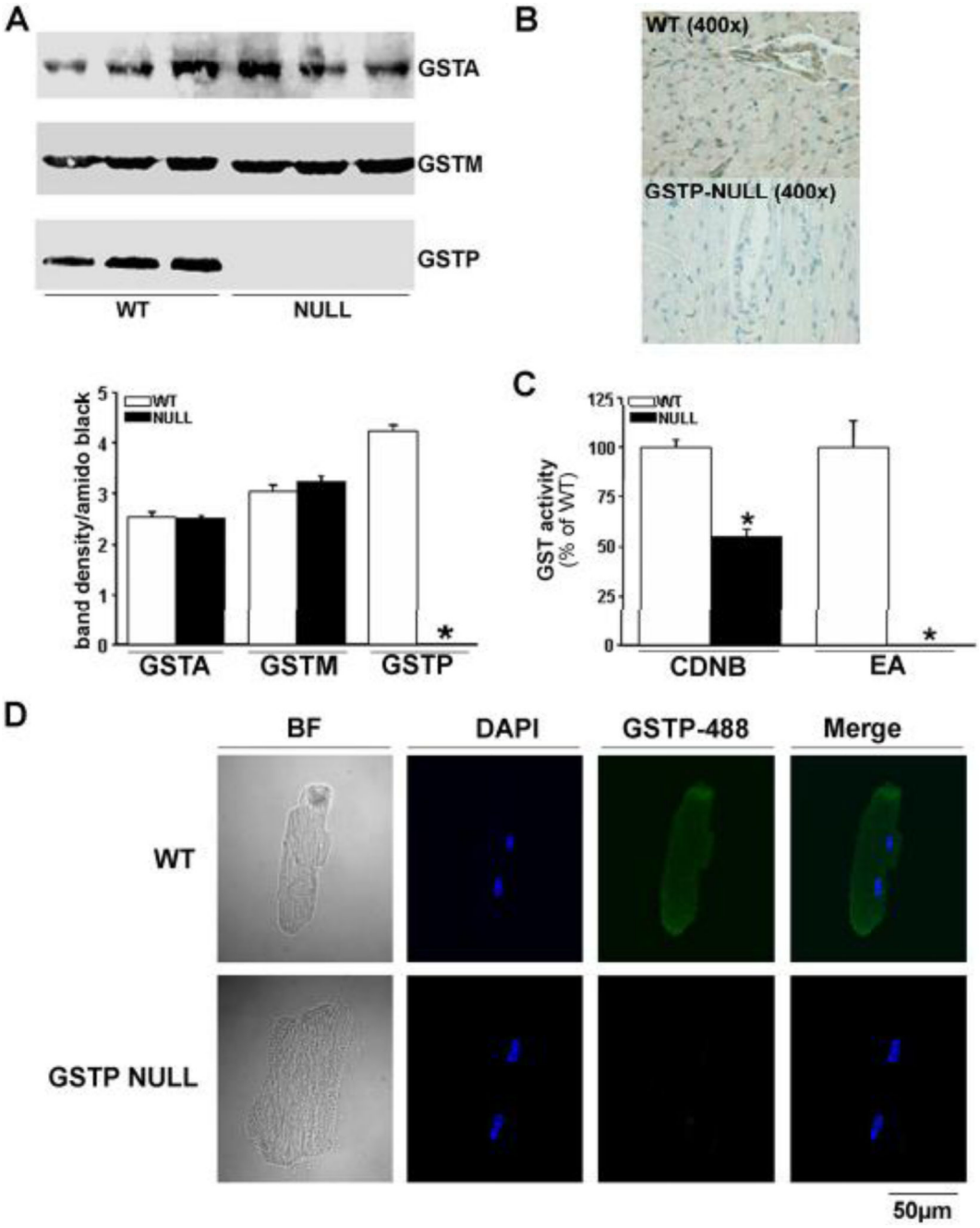

Figure 1. Cardiac distribution of mGstp1/p2 protein and GST activity in WT and GSTP-null mice

(A) Western blots and densitometric analysis (lower panel) of lysates from hearts of WT and GSTP-null mice probed with antibodies against GSTA (α), GSTM (μ) or GSTP (π). (B) Representative photomicrographs of mid-left ventricle cross sections from naïve WT (top) and GSTP-null mice immuno-labeled for GSTP (mag. 400x). (C) Total GST and GSTP-specific activities in cardiac homogenates of WT and GSTP-null mice using 1-chloro-dinitrobenzene (CDNB) and ethacrynic acid (EA) as respective substrates. Specific GSTP immunofluorescence in isolated cardiomyocytes demostrating cytosolic distribution (Fig.

1D). Cardiomyocyte images include (from left to right): differential interference contrast; DAPI only (blue, nuclear staining); GSTP only (488 nm; green); and, overlay DAPI+GSTP. Values are mean ± SEM (* $p<0.05$, GSTP-null vs. WT; N=3 mice/group).

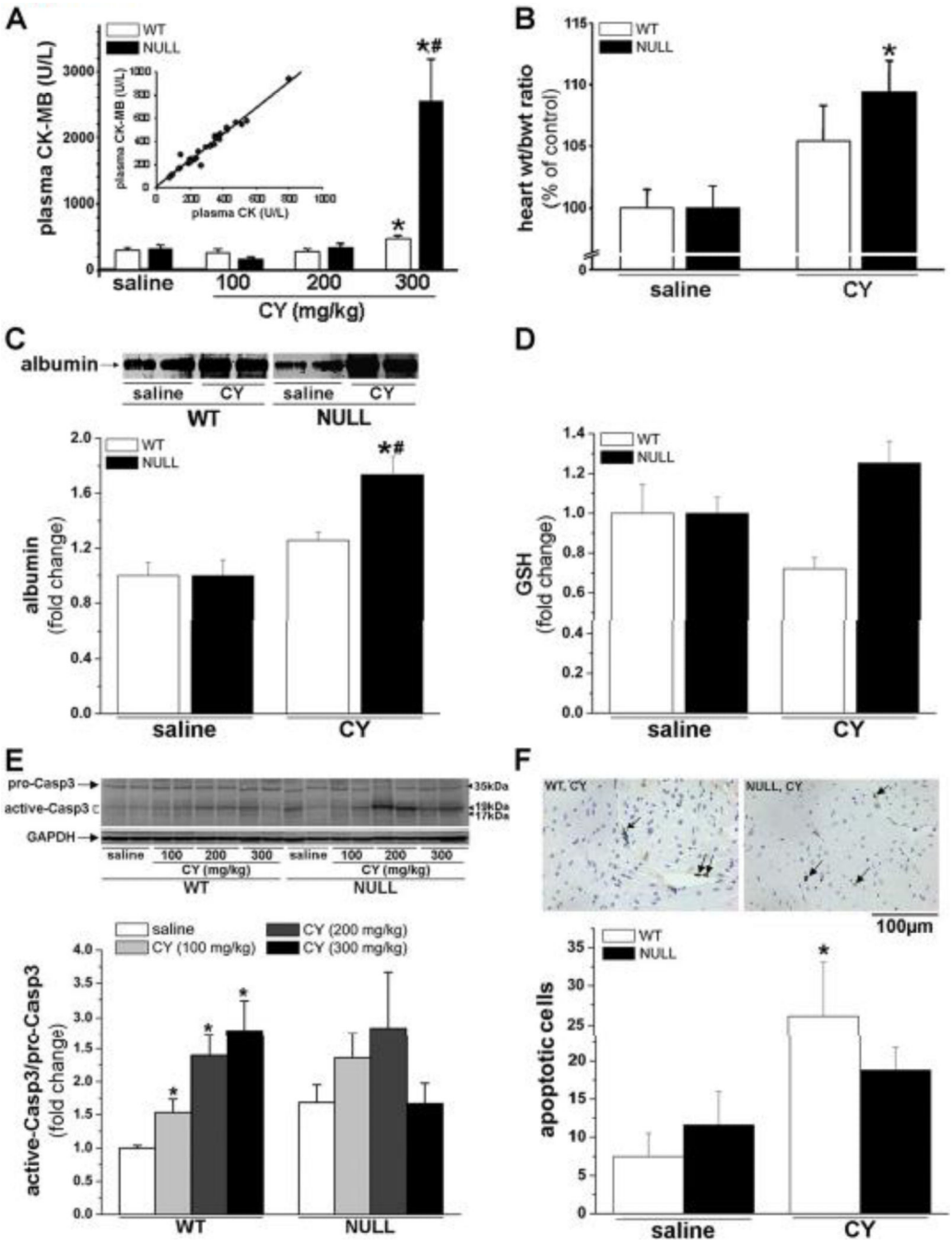

Figure 2. Cyclophosphamide (CY)-induced cardiotoxicity in WT and GSTP-null mice

(A) Plasma creatine kinase-MB (CK·MB) levels in WT and GSTP-null mice 4h after CY (100-300 mg/kg, ip) treatment. Inset: Correlation between plasma CK·MB and CK levels (R^2=0.96). (B) Heart wet weight:body weight ratio in WT and GSTP-null mice 24h post-CY (200 mg/kg) treatment. (C) Western blot analysis of albumin in cardiac lysates of saline or CY-treated WT and GSTP-null mice 4h after dosing. (D) GSH levels in hearts of CY-treated WT and GSTP-null mice 4h after CY (300 mg/kg). (E) Western blots and densitometric analysis of pro- and active caspase-3 in cardiac lysates of mice 4h after CY treatment at

indicated doses. (F) Immunohistochemical staining and quantification of TUNEL positive cells (apoptosis-positive, indicated by arrows) in hearts of WT and GSTP-null mice 4h after saline or CY (200 mg/kg) treatment. Data are mean ± SEM (*p<0.05 vs. matched saline controls; $^{\#}p$<0.05 WT vs. GST-null; N=4-7 mice/group).

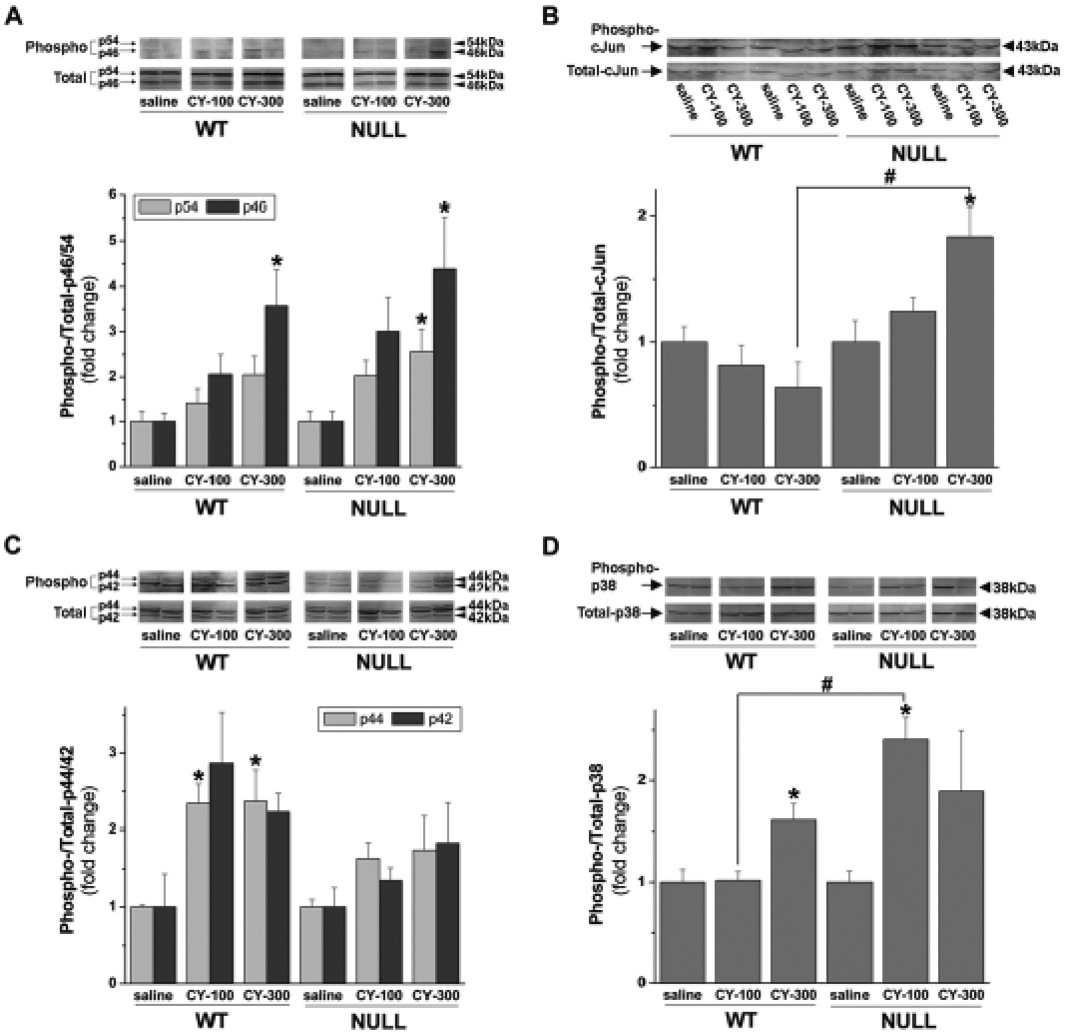

Figure 3. Cyclophosphamide (CY)-induced phosphorylation of JNK, c-Jun, ERK1/2 and p38 in hearts of WT and GSTP-null mice

Representative Western blots and densitometric analyses of (A) phospho-JNK and total JNK (p54/46), (B) phospho-c-Jun and total c-Jun, (C) phospho-ERK and total ERK, and (D) phospho-p38 and total p38 in cardiac lysates from WT and GSTP-null mice 4h after injection of saline or CY (100 or 300 mg/kg, ip). Data are mean ± SEM (*p<0.05; N=4-5 mice/group).

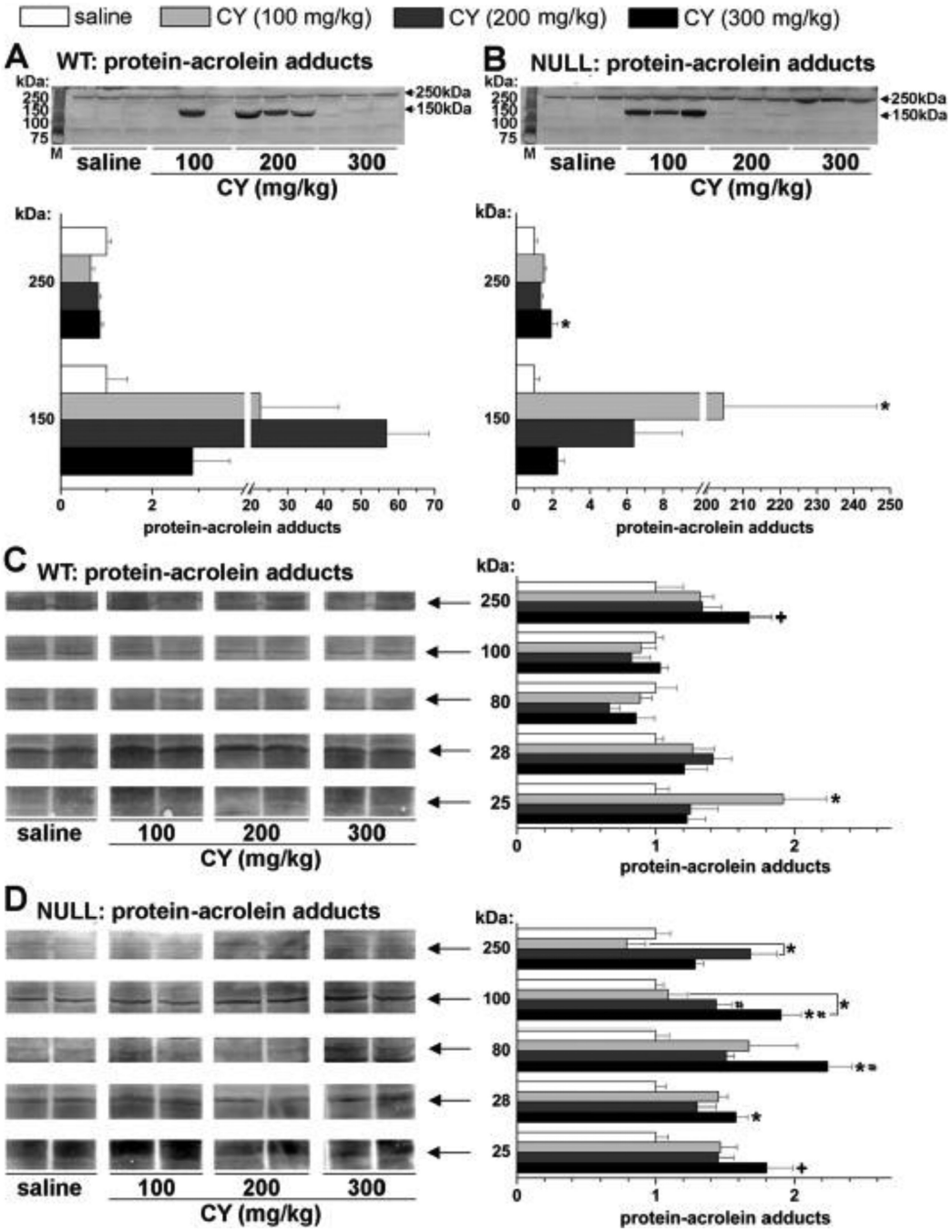

Figure 4. Cardiac abundance of protein-acrolein adducts in cyclophosphamide (CY)-treated WT and GSTP-null mice

Representative Western blots and densitometric analysis of protein-acrolein adducts detected in plasma of (A) WT and (B) GSTP-null mice treated with saline or CY (100, 200 or 300 mg/kg, ip, 4h). Data are mean ± SEM (*p<0.05; saline vs. CY; N=3 mice/group). Western blots and densitometric analyses of discrete protein-acrolein adduct bands in cardiac lysates of (C) WT and (D) GSTP-null mice 4h after treatment with saline or CY (100, 200 or 300

mg/kg, ip). Data are mean ± SEM (*p<0.05 treated vs. matched-control; $^{\#}p$<0.05 GSTP-null vs. matched-WT; + 0.10>p>0.05 treated vs. matched-control; N=5 mice/group).

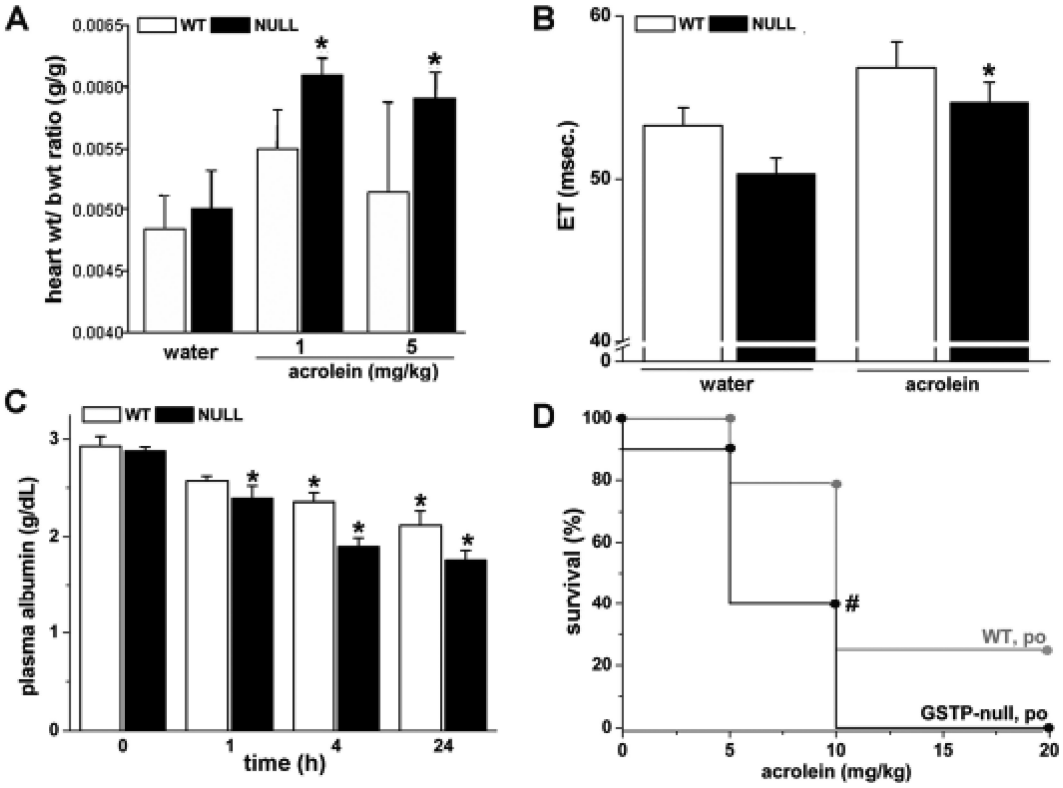

Figure 5. Systemic and cardiac response to acrolein treatment in WT and GSTP-null mice

(A) Heart wet weight:body weight ratio of WT and GSTP-null mice after water or acrolein (1 or 5 mg/kg). (B) Cardiac ejection time (ET, msec) in WT and GSTP-null mice after treatment with acrolein (5 mg/kg, po, 1h). (C) Plasma albumin levels in WT and GSTP-null mice 1, 4, or 24h after administration of water or acrolein (5 mg/kg, po). (D) Mortality (% survival) in WT and GSTP-null mice 24h after treatment with a single dose of 0, 5, 10 or 20 mg/kg acrolein (po). Data are mean ± SEM (*p<0.05; $^{+}$0.10>p>0.05 water vs. acrolein; N≥4 mice/group).

Toxicol Appl Pharmacol. Author manuscript; available in PMC 2016 June 01.

Table 1

Acute echocardiography effects of cyclophosphamide (CY) in WT and GSTP-null mice.

Variable	WT, control	WT, 1h	WT, 4h	Null, control	Null, 1h	Null, 4h
RR	118.7±3.2	101.9±2.8*	106.7±1.7	120.9±3.7	109.5±1.5	105.6±1.2*
HR	508±14	590±16	563±9	500±14	548±7	568±6*
LVIDD	3.82±0.08	4.15±0.30	3.68±0.23	3.90±0.21	3.39±0.32†	3.60±0.28
LVIDS	2.50±0.12	2.74±0.51	2.38±0.24	2.53±0.22	2.11±0.31†	2.06±0.15
EDV	53±3	43±2*	43±4	49±1	36±6	49±8
ESV	22±1	13±2*	12±2	16±1	10±3	15±4
EF	63.4±4.4	70.4±3.4*	70.0±5.1*	67.6±2.6	72.2±3.4†	70.9±3.3
EDA	11.98±0.54	10.96±0.75	10.60±1.25	11.25±0.60	8.97±0.54*	10.18±0.92
ESA	5.93±0.25	3.90±0.65*	4.80±0.83	4.94±0.17	2.97±0.24*	4.31±0.51
FAC	50±2	65±3*	55±5	56±2	67±2*	58±1
ET	46.1±1.9	38.9±1.7†	37.7±1.4	45.8±1.9	38.7±0.7	36.2±2.2*
ETc	51.2±2.0	43.6±1.9†	42.1±1.6	51.0±2.1	43.2±0.7	40.6±2.4*
Vcf	7.59±0.80	9.41±2.29	9.38±1.07	7.88±0.64	9.99±1.17*	11.91±1.00†
Vcfc	22.22±2.63	29.74±7.49	28.78±3.45	22.82±2.03	30.23±3.72*	36.63±2.93†

Echocardiography images were acquired at 1h or 4h after saline (control) or CY treatment (300 mg/kg bwt, ip). Abbreviations (units): WT, wild-type; Null, GSTP-null; RR, R-R interval (msec); HR, heart rate (bpm); LVIDD, left ventricle internal diameter diastole (mm); LVIDS, left ventricle internal diameter systole (mm); EDV, end diastolic volume (μl); ESV, end systolic volume (μl); EF, ejection fraction (%, [(EDV-ESV)/EDV*100]); EDA, end diastolic area (mm^2); ESA, end systolic area (mm^2); FAC, fractional area change (%,[(EDA-ESA)/EDA*100]); ET, ejection time (msec); ETc, ejection time (msec; corrected); Vcf, velocity circumferential fiber shortening (circ/s); Vcfc, velocity circumferential fiber shortening (heart rate corrected; Vcf/ETc*100). Data are mean ± SEM

*$p<0.05$ vs. baseline

†$0.10>p>0.05$ vs. matched control; N=3-6 mice/group.

Table 2

Hemodynamic effects of cyclophosphamide in WT and GSTP-null mice.

WT	**Baseline**	**CY**
Blood Pressure		
Systolic (mmHg)	110.2±1.1	107.6±0.9*
Mean (mmHg)	93.6±0.9	82.8±1.1*
Diastolic (mmHg)	85.6±0.8	71.0±1.2*
Heart Rate (bpm)	750±3	653±5*
GSTP-null	**Baseline**	**CY**
Blood Pressure		
Systolic (mmHg)	119.6±0.6	112.7±0.7*
Mean (mmHg)	104.1±0.6	92.9±1.0*
Diastolic (mmHg)	96.8±0.7	83.5±1.2*
Heart Rate (bpm)	720±3	703±5

Blood pressure and heart rate were measured by non-invasive tail cuff pressure-volume plethysmography at 4h after CY treatment (200 mg/kg bwt; ip). Data are mean ± SEM

*$p<0.05$ vs. baseline; N=5-6 mice/group.

Table 3

Mass spectrometry-based identification of proteins from mouse cardiac lysate following acute cyclophosphamide treatment (CY, 300 mg/kg; 4h) immunoprecipitated using a polyclonal protein-acrolein antibody.

Identified Proteins (20)	Uniprot Accession #	Mol. Wt.	Function/Source
Kallikrein 1-related peptidase*	K1B22_MOUSE	28 kDa	serine protease
Kallikrein 1-related peptidase*	K1B26_MOUSE	28 kDa	serine protease
Serum albumin (Fragment)	G5B5P2_HETGA	68 kDa	plasma protein
Dermcidin	Q71DI1_RAT	11 kDa	antimicrobial/sweat glands
Kallikrein 1-related peptidase	K1B11_MOUSE	29 kDa	serine protease
Kallikrein 1-related peptidase	K1KB9_MOUSE	29 kDa	serine protease
Myoglobin	MYG_ONDZI	17 kDa	O_2 binding
Uncharacterized protein	D3ZDF6_RAT	12 kDa	unknown
Uncharacterized protein	I3MYH6_SPETR	62 kDa	unknown
Interferon-induced very large GTPase 1	G3IH28_CRIGR	279 kDa	binds/cleaves GTP
HEAT repeat-containing protein 1	G5APM6_HETGA	237 kDa	alpha-helical pair
Uncharacterized protein	I3MMW4_SPETR	48 kDa	unknown
Serum albumin	ALBU_MESAU	68 kDa	plasma protein
Uncharacterized protein	I3LW34_SPETR	53 kDa	unknown
Meiosis inhibitor protein 1	F8WHB9_MOUSE	147 kDa	testis
Uncharacterized protein (Fragment)	F1M111_RAT	202 kDa	unknown
Transgelin-2	G5AMF2_HETGA	20 kDa	actin binding
Uncharacterized protein	H0UT44_CAVPO	164 kDa	unknown
Kallikrein 1-related peptidase*	K1B16_MOUSE	29 kDa	serine protease
Lactoperoxidase	Q5SW46_MOUSE	80 kDa	antibacterial, saliva/mucus

*Proteins with high confidence MS/MS assignment of protein acrolein adducts to K, C, or H residues.

Table 4

Hemodynamic effects of acrolein treatment in WT and GSTP-null mice.

WT		**Acrolein**	
	Baseline	**1**	**3**
Blood Pressure		(Δ from baseline)	
Systolic (mmHg)	109.4±0.5	−0.4±3.2	−13.9±9.7*
Mean (mmHg)	90.4±0.3	−3.4±3.6	−18.6±10.1*
Diastolic (mmHg)	81.0±0.3	−4.9±3.9	−20.8±10.3*
Heart Rate (bpm)	726±2	−4±28	+3±38
GSTP-null		**Acrolein**	
	Baseline	**1**	**3**
Blood Pressure		(Δ from baseline)	
Systolic (mmHg)	112.5±1.2	+5.0±8.4	−20.3±14.2*
Mean (mmHg)	96.8±1.1	+2.4±8.9	−27.7±15.4*
Diastolic (mmHg)	89.4±1.1	+1.1±9.2	−31.7±16.6*
Heart Rate (bpm)	678±7	−46±19	+15±26

Blood pressure and heart rate were measured by non-invasive tail cuff pressure-volume plethysmography 1h after treatment with indicated acrolein dose (mg/kg bwt, ip). Data are mean ± SEM

* $p<0.05$, paired *t*-test vs. matched baseline control; N=5-6 mice/group for WT; N=3-5 mice/group for GSTP-null.

Table 5

Effect of acrolein treatment on organ level of reduced glutathione (GSH).

		Time (h)		
	Baseline	**1**	**4**	**24**
WT		% baseline		
Heart	1.69±0.33	127.3±7.3*	107.4±15.4	82.0±13.0
Stomach	3.67±0.22	63.8±4.4*	74.8±4.5	75.4±7.0
Liver	6.74±0.16	106.0±4.2	87.3±6.6	104.4±6.7
GSTP-null		% baseline		
Heart	1.93±0.31	81.3±5.8†	108.1±4.3	83.0±11.0
Stomach	5.14±0.90	53.5±4.0*	103.1±6.9	74.9±8.4
Liver	7.47±0.29	100.6±6.2	95.9±8.0	104.4±6.7

Acrolein exposure was 5 mg/kg bwt (p.o.). Baseline GSH level is μmol GSH/g tissue wet weight. GSH values are presented as a percentage of baseline at post-acrolein treatment points. Data are mean ± SEM

*$p<0.05$ vs. baseline

†$0.10>p>0.05$ vs. baseline; N=6-8 mice/group.